Localization and Kinetics of Protein Kinase C-Epsilon Anchoring in Cardiac Myocytes

Seth L. Robia, Jyothi Ghanta, Valentin G. Robu, and Jeffery W. Walker
Department of Physiology, University of Wisconsin, Madison, Wisconsin 53706 USA

ABSTRACT Protein kinase C-ϵ (PKC-ϵ) plays a central role in cardiac cell signaling, but mechanisms of translocation and anchoring upon activation are poorly understood. Conventional PKC isoforms rely on a rapid Ca^{2+}-mediated recruitment to cell membranes, but this mechanism cannot be employed by PKC-ϵ or other PKC isoforms lacking a Ca^{2+}-binding domain. In this study, we used recombinant green fluorescent protein (GFP) fusion constructs and confocal microscopy to examine the localization, kinetics, and reversibility of PKC-ϵ anchoring in permeabilized rat cardiac myocytes. PKC-ϵ-GFP bound with a striated pattern that co-localized with α-actinin, a marker of the Z-line of the sarcomere. Binding required activation of PKC and occurred slowly but reversibly with apparent rate constants of $k_{on} = 4.6 \pm 1.2 \times 10^3\ M^{-1}\ s^{-1}$ and $k_{off} = 1.4 \pm 0.5 \times 10^{-3}\ s^{-1}$ ($t_{1/2} = 8$ min) as determined by fluorescence recovery after photobleaching and by perfusion experiments. A truncated construct composed of the N-terminal 144-amino-acid variable region of PKC-ϵ (ϵV_1-GFP), but not an analogous N-terminal domain of PKC-δ, mimicked the Z-line decoration and slow binding rate of the full-length enzyme. These findings suggest that the ϵV_1 domain is important in determining PKC-ϵ localization and translocation kinetics in cardiac muscle. Moreover, PKC-ϵ translocation is not a diffusion-controlled binding process but instead may be limited by intramolecular conformational changes within the V_1 domain. The k_{off} for ϵV_1-GFP was two- to threefold faster than for full-length enzyme, indicating that other domains in PKC-ϵ contribute to anchoring by prolonging the bound state.

INTRODUCTION

Protein kinase C (PKC) is widely recognized as a central regulatory species in a variety of physiological systems. At least 11 distinct PKC isoforms have been identified by molecular and biochemical analysis (Nishizuka, 1992). The conventional PKC (cPKC) isoforms α, βI, βII, and γ are regulated by phosphatidylserine, diacylglycerol, and Ca^{2+}. More recently, several novel PKC (nPKC) isoforms ϵ, δ, η, and θ have been shown to be Ca^{2+} independent and regulated primarily by phosphatidylserine and diacylglycerol. PKC typically undergoes redistribution from one intracellular region to another upon stimulation by various intracellular signaling factors, including diacylglycerol, fatty acids, and in the case of the cPKC isoforms, calcium. This translocation effect occurs over the course of seconds to minutes, with each isoform exhibiting a characteristic pattern and time course of redistribution (Disatnik et al., 1994; Jaken, 1996; Kiley et al., 1995). The mechanism of this enzyme translocation and anchoring has been most widely investigated for conventional PKC isoforms, which seem to translocate and partition rapidly into cell membranes through a Ca^{2+}-binding C_2 domain. PKC isoforms thought to be important in modulating cardiac contractility include novel isoforms, PKC-ϵ and PKC-δ, which lack this Ca^{2+}-binding C_2 domain and are therefore likely to translocate by a distinct mechanism.

The ϵ isoform of PKC has garnered considerable scrutiny in cardiac signaling because of its association with ischemic preconditioning (IP), a phenomenon wherein a temporary period of reduced blood flow confers protection against a subsequent prolonged ischemic insult (Murry et al., 1986; Albert and Ford, 1999; Kawamura et al., 1998; Ping et al., 1997; Qiu et al., 1998). Of particular interest is the suggestion that a delay in the onset of cardioprotection is due to the time taken for PKC-ϵ translocation and that the memory of preconditioning is due to PKC dwelling in a translocated state (discussed in Cohen et al., 2000, and sources therein). This provides a compelling reason to establish the mechanism and kinetics of PKC-ϵ translocation in the heart.

The evidence linking translocation to regulation of contractility or to cardioprotection fosters a great interest in the mechanism by which PKC exerts its effects, and efforts have been made to identify important activators, anchoring proteins, and target substrates. Previous fluorescence immunolabeling studies in the heart showed PKC-ϵ binding in a striated, sarcomeric pattern visible by epifluorescence and confocal microscopy (Disatnik et al., 1994; Huang et al., 1997). Binding of PKC-ϵ to Golgi structures, cell-cell contacts, perinuclear regions, and intercalated disks has also been reported in cardiac tissues (Csukai et al., 1997; Wang and Ashraf 1998). Certain phases of PKC-ϵ translocation occur in the time domain of 5–20 min (Huang et al., 1997), but the steps in the signaling cascade responsible for this slow rate have not been identified.

To better understand the Ca^{2+}-independent translocation and anchoring of the novel PKC-ϵ isoform, we have examined the binding and dissociation properties of purified green fluorescent protein (GFP) fusion constructs applied to isolated permeabilized rat cardiac myocytes. The use of

Received for publication 21 November 2000 and in final form 16 February 2001.

Address reprint requests to Dr. Jeffery W. Walker, Department of Physiology, 1300 University Avenue, Madison, WI 53706. Tel.:608-262-6941; Fax: 608-265-5512; E-mail: jwalker@physiology.wisc.edu.

0006-3495/01/05/2140/12 $2.00

permeabilized cells permitted the concentration of fluorescent probes to be known and readily varied over a wide range. A major advantage of this approach over immunolocalization techniques is that binding can be monitored over time with confocal microscopy, allowing determination of dynamic parameters such as on/off rates and equilibrium binding constants. This study provides the first estimates of these dynamic parameters for PKC-ϵ binding near the Z-line of cardiac cells.

MATERIALS AND METHODS

All reagents were obtained from Sigma Chemical Co. (St. Louis, MO) unless noted otherwise. Phorbol 12-myristate 13-acetate (PMA) and 4-α-phorbol-didecanoate (4-α-PDD) were obtained from Calbiochem (La Jolla, CA) and prepared as 1 mM stock solutions in dimethylsulfoxide. Collagenase was obtained from Worthington Enzymes (Freehold, NJ).

Cardiac myocyte preparation

Ventricular cardiac myocytes were isolated from adult male Sprague-Dawley rats by enzymatic digestion with collagenase and hyaluronidase, as previously described (Huang et al., 1996). Myocytes were then permeabilized with 100 μg/ml saponin for 5 min at 20°C in relaxing solution of the following composition: 100 mM KCl, 1 mM $MgCl_2$, 2 mM EGTA, 4.5 mM ATP, 10 mM imidazole, 1 mM dithiothreitol, pH 7.0. Cells were washed and resuspended in relaxing solution containing 5% bovine serum albumin to block nonspecific binding of applied probes.

Molecular biology and protein expression

A PKC-ϵ-GFP fusion protein was expressed in SF-9 or SF-21 insect cells using a commercial baculovirus expression system Fastbac1 (GibcoBRL-Life Technologies, Gaithersburg, MD). The enhanced-GFP gene was excised from pEGFP-C1 (Clontech, Palo Alto, CA) and inserted into a previously engineered plasmid 5′ to the gene encoding PKC-ϵ. This plasmid, derived from the Life Technologies pFASTBAC vector, undergoes recombination in DH10Bac cells, making a bacmid suitable for insect cell transfection. PKC was purified from insect cell lysates using a Vision purification system (PE Biosystems, Foster City, CA) equipped with rapid perfusion anion exchange columns. The fusion protein thus produced was enzymatically active and regulated by the PKC activator phorbol 12-myristate 13-acetate (PMA) as determined by a commercially available assay, MESACUP protein kinase assay kit (Pan Vera, Madison, WI). The specific activity of PKC-ϵ-GFP was determined by [^{32}P]phosphate incorporation into myelin basic protein using a previously described enzymatic assay (Huang et al., 1996). PMA-dependant activity was found to be 28 U/mg protein (where 1 U = 1 nmol of phosphate transferred per minute), with a PMA-independent basal activity of 4 U/mg protein. This is similar to the specific activity of commercially available PKC-ϵ (Panvera, Madison, WI), which had a PMA-dependent activity of 60 U/mg protein, under the same assay conditions.

The V_1 regions of PKC-ϵ and PKC-δ were amplified from a mouse brain cDNA library (Stratagene, La Jolla, CA) by the polymerase chain reaction (PCR) and inserted into pEGFP (Clontech). The ϵV_1-GFP construct contained a histidine-tag sequence and was purified from DH5-α *Escherichia coli* cell lysate using a column of Ni-NTA Superflow beads (Qiagen, Valencia, CA). The δV_1-GFP fusion gene was subcloned into pGEX-2T (Amersham Pharmacia, Piscataway, NJ) and expressed as a glutathione-S-transferase (GST)-tagged protein. After purification with glutathione Sepharose 4B beads (Amersham), the GST tag was removed by thrombin cleavage.

Confocal microscopy

Imaging was performed with a Bio-Rad MRC 1024 laser scanning confocal microscope equipped with a mixed gas (Ar/Kr) laser operated by 24-bit LaserSharp software. Image acquisition in the green channel utilized excitation at 488 nm with emission detected at 522 ± 17 nm. Acquisition in the red channel utilized excitation at 568 nm with emission detected at 605 ± 16 nm. Immunolabeling of α-actinin was performed with a commercial monoclonal antibody EA-53 (Sigma Immunochemical, St. Louis, MO) diluted 1:100, and anti-mouse IgG secondary antibody labeled with tetramethyl-rhodamine isothiocyanate (TRITC) (Boehringer Mannheim, Indianapolis, IN) or Alexa 568 (Molecular Probes, Eugene, OR) diluted 1:50. GFP fusion constructs were applied at 200–600 nM for localization studies. PKC-ϵ-GFP was activated by preincubation in relaxing solution containing stoichiometric concentrations of PMA, except where indicated. The ϵV_1-GFP construct does not contain the C_1 domain implicated in phorbol ester binding (Ono et al., 1989) and was not treated with exogenous activators in these experiments.

Heat denaturation control experiments were performed by dilution of PKC-ϵ-GFP in relaxing solution followed by incubation at 70°C for 10 min. This treatment did not significantly affect the fluorescence of GFP constructs consistent with the fact that GFP itself possesses considerable thermal stability (Ward et al., 1982).

Photobleaching of saponin-permeabilized myocytes decorated with GFP constructs was performed by increasing laser power from 30% to 100% and enhancing scan zoom by a factor of 10. This increased the intensity of laser illumination by >300-fold, destroying GFP chromaphores in a region measuring 16 μm × 16 μm. Fluorescence recovery was then observed by acquiring single images at 1-min intervals for 20 min. Image analysis was performed with Scion Image (Scion Corp., Frederick MD), Confocal Assistant (Bio-Rad, Hercules, CA), and Metamorph (Universal Imaging Corp., West Chester, PA). Fluorescence intensity plots were generated from confocal images using these programs to draw straight scan paths parallel to the long axis of the cell. The paths thus intersected the repetitive striations, yielding a multiply peaked trace that was analyzed manually and automatically with a custom peak height detection program developed by Dr. K. S. Campbell, University of Wisconsin Department of Physiology. This program identified peaks in the fluorescence intensity/position plot based on local maxima and minima that satisfy designated threshold criteria. The program determined and displayed the mean peak height (±SD) and mean fluorescence intensity (±SD).

In PKC-ϵ-GFP washout experiments, isolated, permeabilized myocytes were settled onto the glass coverslip floor of a custom perfusion chamber and decorated with 50–100 nM PKC-ϵ-GFP. After probe equilibration, the cells were perfused with fresh buffer using a peristaltic pump (Scientific Industries, Bohemia, NY) and monitored by confocal microscopy, acquiring one frame every 30 s for 1–2 h. The amount of PKC-ϵ-GFP bound was evaluated at each time point as the average fluorescence of a rectangular section. In some cases, individual cells were held in place on the surface of the coverslip using a stainless steel probe mounted on a micro-manipulator apparatus (Narishige, Tokyo, Japan) to prevent cells from shifting position during rapid solution changes.

Kinetic measurements

Time courses of binding and unbinding were determined quantitatively by monitoring the fluorescence intensity within myocytes or within the 16-μm × 16-μm bleached region over the entire acquisition period. Fluorescence intensity time courses were fit to single exponentials to obtain first-order rate constants that were consistent with the independent measure of rates by visual inspection. Half-time values estimated for striation development or photobleaching recovery were consistent between three observers blinded to sample identity. Half-times were converted to observed rate constants by $k = (\ln 2)/t_{1/2}$.

RESULTS

Localization of activated PKC-ϵ−GFP

Recombinant PKC-ϵ-GFP was incubated with saponin-skinned myocytes to determine the subcellular location of PKC-ϵ binding in heart myocytes. In the absence of activators, PKC-ϵ-GFP stained only at low levels and diffusely throughout the cells (Fig. 1 *A*). Activation with 100 nM PMA increased binding of PKC-ϵ-GFP to longitudinal structures as well as the perinuclear region (Fig. 1 *B*). Inclusion of 100 nM Zn^{2+} plus 100 nM PMA provided the most reproducible staining pattern characterized by promi-

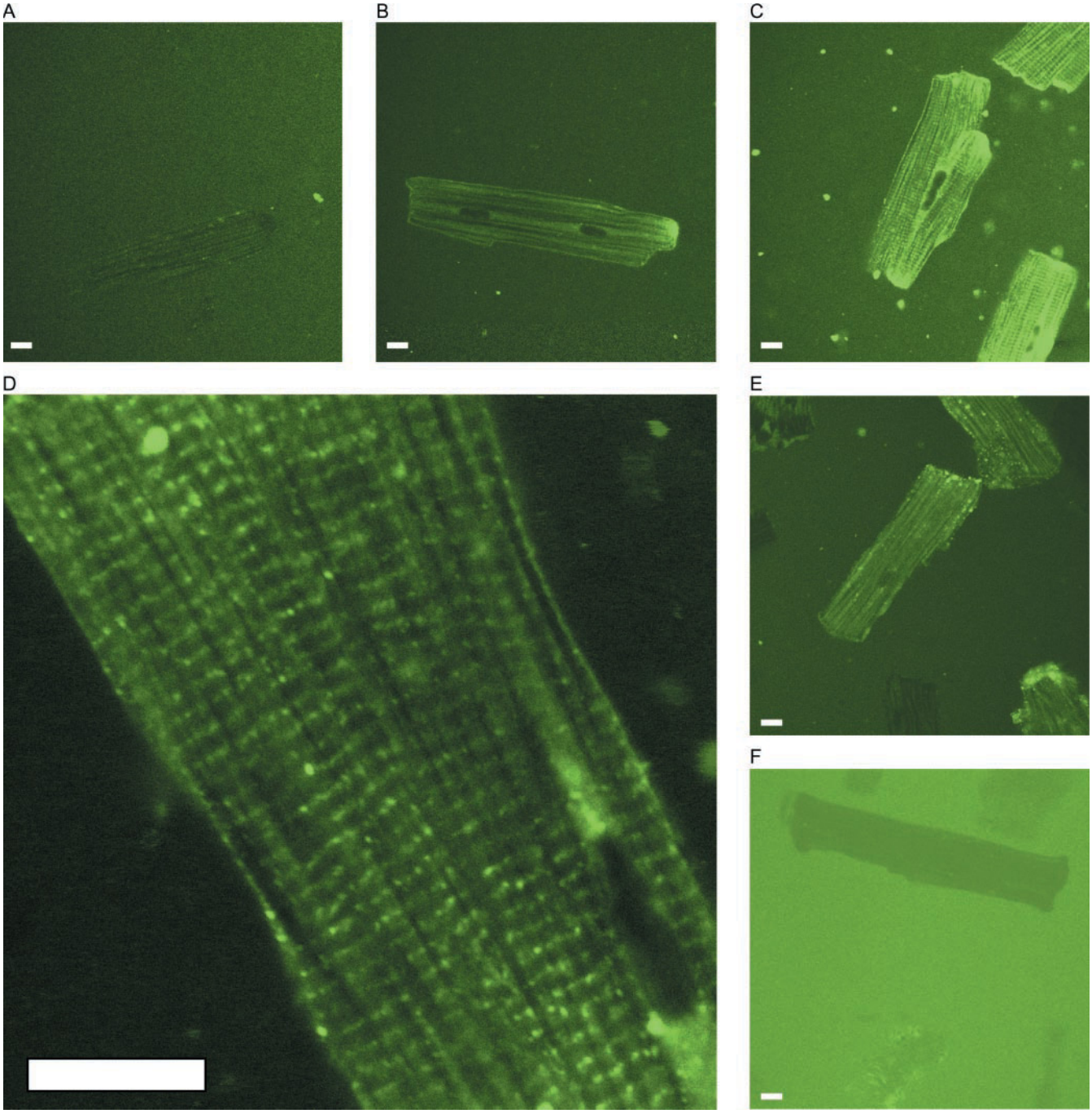

FIGURE 1 Confocal images of isolated permeabilized myocytes after incubation with 100 nM PKC-ϵ-GFP. (*A*) PKC-ϵ-GFP in relaxing solution with no activators; (*B*) PKC-ϵ-GFP plus 100 nM PMA; (*C*) PKC-ϵ-GFP plus 100 nM PMA plus 100 nM $ZnCl_2$; (*D*) As in *C*, a higher magnification image averaged from three sequential acquisitions; (*E*) PKC-ϵ-GFP plus 100 nM $ZnCl_2$ plus 100 nM 4-α-PDD, a biologically inactive phorbol ester; (*F*) 400 nM EGFP not fused to PKC. Scale bars, 10 μm.

nent decoration of intercalated disks and a pronounced cross-striated staining pattern (Fig. 1, *C* and *D*). Nanomolar levels of Zn^{2+} are presumably required for proper folding and function of the C1 domains containing zinc fingers. Only active PKC-ϵ-GFP bound, as no staining was observed in the presence of the inactive phorbol ester, 4-α-PDD (Fig. 1 *E*), and normal binding was prevented by heat denaturation of PKC-ϵ-GFP (70°C, 10 min; not shown). Moreover, EGFP itself did not bind to myocytes significantly, as no decoration of cross-striations or of intercalated disks was observed with unconjugated EGFP (Fig. 1 *F*). In these images with EGFP alone, cells appear darker than the bath in part because the saponin permeabilization technique is selective for the plasma membrane (Endo and Iino 1980), and therefore intracellular membrane compartments such as mitochondria and the sarcoplasmic reticulum are inaccessible to freely diffusible EGFP.

The intensity of bound PKC-ϵ-GFP fluorescence varied with protein concentration over the range 20–160 nM. Due to limits on attaining higher concentrations of PKC-ϵ-GFP, we were unable to demonstrate saturation of binding to intercalated disks or to cross-striated structures. The saturability and specificity of binding were confirmed by preincubation of myocytes with activated unlabeled PKC-ϵ (3 μM protein plus 200 nM PMA), which reduced the proportion of fluorescent striated cells from >40% to <10% (data not shown). Overall the data are consistent with the notion that upon activation PKC-ϵ preferentially anchors to specific cross-striated structures and intercalated disks in cardiac myocytes. This staining pattern including the exclusion of PKC-ϵ-GFP from the nucleus is similar to what was observed previously by immunofluorescence (Huang et al., 1997).

To further establish the localization of activated PKC-ϵ-GFP we compared the staining pattern with the localization of α-actinin, a structural protein recognized to be a marker of the Z-line region of the sarcomere. Fig. 2 (*left panel*) shows the pattern obtained with a commercial polyclonal antibody to α-actinin detected by an Alexa 568-labeled secondary antibody. The middle panel of Fig. 2 illustrates a typical PKC-ϵ-GFP image, and the right panel merges the GFP and Alexa 568 channels to highlight regions of overlap. Yellow regions in the merged image demonstrate clear co-localization of activated PKC-ϵ-GFP with α-actinin. Decoration of the Z-line was analyzed in the remainder of this study because it was more amenable to quantification and was quite reproducible from cell to cell.

FRAP of PKC-ϵ-GFP

Fluorescence recovery after photobleaching (FRAP) measurements were employed to measure the kinetics of PKC-ϵ binding and unbinding. FRAP has the advantage that cells are premixed with PKC-ϵ-GFP and allowed to fully equilibrate before the bleaching perturbation. Fig. 3 *A* illustrates the recovery of striations in a square bleached region of permeabilized myocytes decorated with PKC-ϵ-GFP. Estimates for photobleaching recovery rates were obtained by two separate approaches (details in Materials and Methods) that gave results in close agreement.

The rate of photobleaching recovery was found to depend on the concentration of PKC-ϵ-GFP applied to the cells. Fig. 3 *B* shows that k_{FRAP} increases with increasing concentration of PKC-ϵ-GFP. The recovery of striations from photobleaching implies PKC-ϵ-GFP binds reversibly and thus equilibrates dynamically between bound and free states as shown in the simple scheme below:

$$\text{Anchoring site} + \text{PKC-}\epsilon\text{-GFP}_{\text{free}} \underset{k_{\text{on}}}{\overset{k_{\text{off}}}{\rightleftharpoons}} \text{PKC-}\epsilon\text{-GFP}_{\text{bound}}$$

In the photobleaching experiments, the rate of recovery of a bleached region is determined by both the binding and unbinding rate constants, because bound, bleached mole-

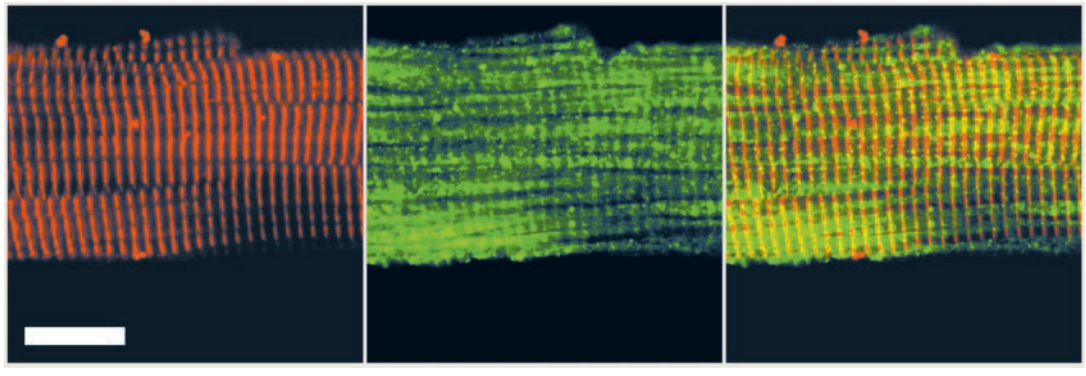

FIGURE 2 Co-localization of activated PKC-ϵ-GFP with the Z-line of cardiac myocytes. (*Left panel*) A confocal image of isolated permeabilized myocytes decorated with a monoclonal anti-α-actinin antibody and Alexa 568-labeled secondary antibodies detected in the red channel; (*Middle panel*) The same cardiac myocyte decorated with activated PKC-ϵ-GFP detected in the green channel. (*Right panel*) Regions of overlap between the two fluorescence channels containing α-actinin and PKC-ϵ-GFP, respectively, are illustrated in yellow.

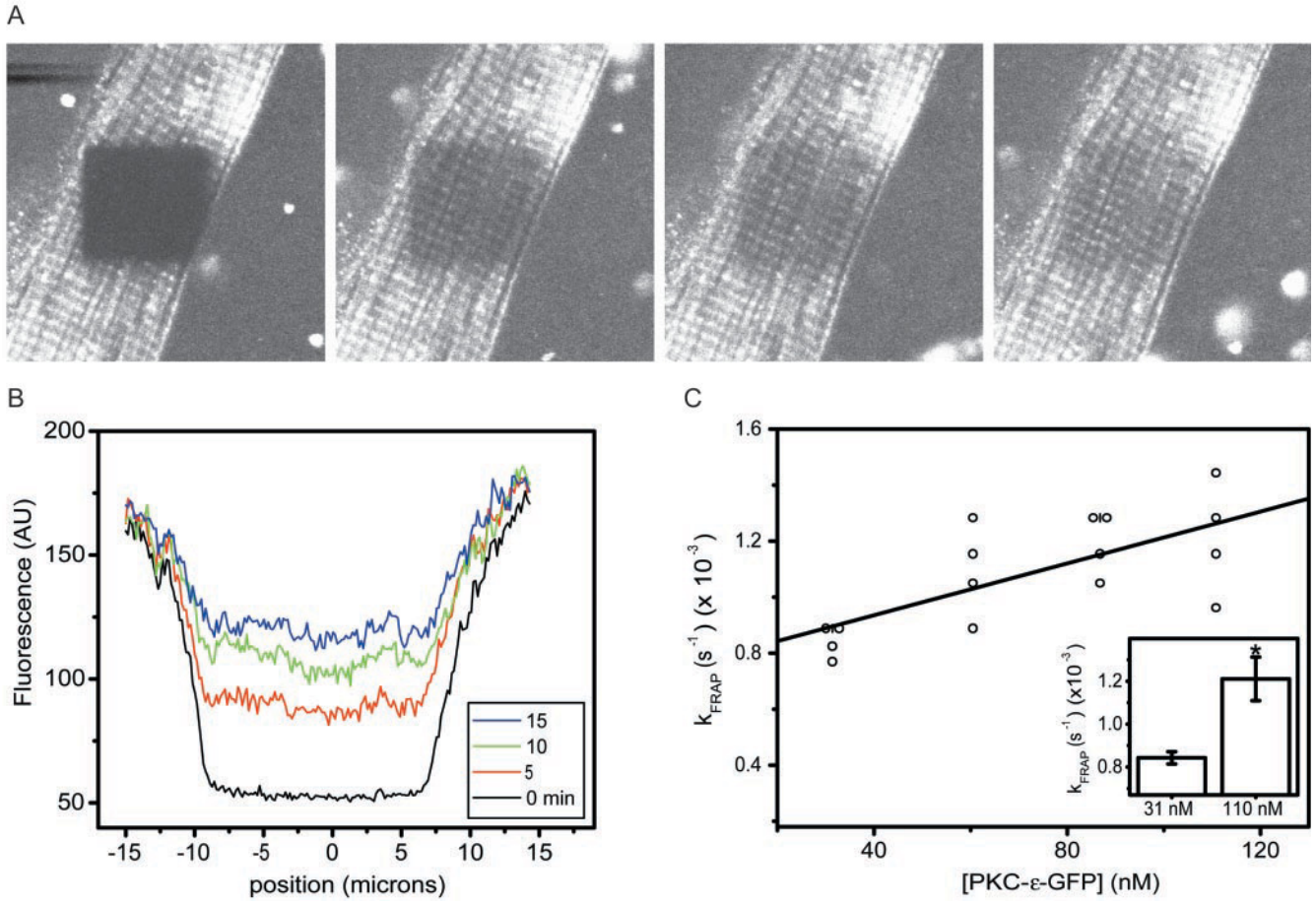

FIGURE 3 Photobleaching recovery of myocytes decorated with PKC-ϵ-GFP. (*A*) A permeabilized myocyte equilibrated with 150 nM activated PKC-ϵ-GFP was photobleached in a 16 × 16 μm square. Recovery of the striation pattern is shown here in four panels at 0, 5, 10, and 15 min after photobleaching. (*B*) A line-scan quantification of fluorescence intensity versus position across the bleached region shows a uniform recovery of fluorescence over time. (*C*) Dependence of the rate of photobleaching recovery, k_{FRAP}, upon the concentration of applied probe. A linear regression fit gave a slope, $k_{on} = 4.6 \pm 1.2 \times 10^3$ $M^{-1}s^{-1}$, and *y*-intercept, $k_{off} = 0.75 \pm 0.10 \times 10^{-3}$ s^{-1}. Overlapping data are offset. (*Inset*) Mean k_{FRAP} values ± SEM at low (31 nM) and high (110 nM) concentrations of PKC-ϵ-GFP. Data are represented as mean ± SEM; asterisk indicates statistical significance with $p < 0.05$.

cules of PKC-ϵ-GFP must vacate binding sites for unbleached species to bind from the available pool in free solution. Consequently, the recovery rate constant, k_{FRAP}, is an integrated measure of k_{on} and k_{off} as follows: $k_{FRAP} = k_{on}$ [PKC-ϵ-GFP] + k_{off}. In this relationship, only k_{on} is in a concentration-dependent term, and thus one observes k_{FRAP} over a range of concentrations to dissect k_{on} from k_{off}. The linear regression in Fig. 3 *B* gives a slope, $k_{on} = 4.6 \pm 1.2 \times 10^3$ M^{-1} s^{-1} and a *y*-intercept, $k_{off} = 0.75 \pm 0.1 \times 10^{-3}$ s^{-1}. The affinity can be determined from these values according to their relationship to the dissociation constant as follows: $K_d = k_{off}/k_{on}$. By this analysis, the apparent K_d for PKC-ϵ-GFP was found to be 160 nM.

Probe diffusion

Importantly, the low k_{on} values reported above argue against a diffusion-limited binding process. It is interesting to note that areas of the photobleaching square that overhang the edge of the cell do not cause any detectable bleaching of fluorescence in the extracellular bath solution (seen best in left image of Fig. 3 *A*), because the bleached area in free solution recovers immediately. Thus, diffusion in free solution is much faster than the formation of the striation staining pattern. This is consistent with the observation that the 16-μm × 16-μm bleached region does not change size or shape during the recovery process. If recovery of the striation pattern were determined by the diffusion rate, then the pattern would be expected to close in from the perimeter of the bleached region. This was not observed, but rather recovery of striations was uniform across the bleached square. This is demonstrated graphically in Figs. 3 *B* and 8 *B*. Line-scan fluorescence quantification traces across the bleached area maintain a characteristic square-stepped shape throughout the recovery process, indicating uniform recovery of fluorescence. Additional analyses show that the

corners of the bleached area recover with the same time dependence as the center (not shown).

Additional control experiments were performed to address whether the saponin-permeabilized plasma membrane presented a barrier to diffusion, using unconjugated EGFP as a freely diffusible probe. As shown in Fig. 1 *F*, the fluorescence signal of EGFP in permeabilized cells is low. To distinguish EGFP from background autofluorescence, a region of the cell was pre-bleached before application of probe. Fluorescence of this region was monitored and compared with an extracellular reference as EGFP was perfused into the bath. The fluorescence increase in the intracellular region followed the rise in extracellular fluorescence without a detectable delay, indicating that the permeabilized membrane did not measurably impede probe access to intracellular regions on the time scale of the frame acquisition rate (one every 15 s).

These empirical observations are in harmony with theoretical predictions of diffusion parameters and photobleaching recovery in this experimental context. Green fluorescent protein has been determined to have a free-solution diffusion coefficient of 8.7×10^{-7} cm^2 s^{-1} (Brown et al., 1999; Swaminathan et al., 1997). Adjusting for the increased Stokes' hydrodynamic radius of the largest construct, PKC-ϵ-GFP, yields a diffusion coefficient on the order of 5×10^{-7} cm^2 s^{-1}. This value gives a theoretical half-time of photobleaching recovery of 0.29 s for a bleached area of radius 8 μm, according to the relationship $t_{1/2} = 0.224\, w^2/D$ where w is bleach radius (Soumpasis 1983). Even if the mobility of the applied probes is significantly hindered by subcellular structures such as the sarcoplasmic reticulum, mitochondria, and myofilaments, as has been demonstrated in similar systems (Papadopoulos et al., 2000, and references therein), the recovery should still be over seconds or tens of seconds. Thus, the observed long photobleaching recovery times, measured in minutes, cannot be due to slow diffusion of fluorescent probes.

PKC-ϵ-GFP binding kinetics by wash-in/washout

FRAP measurements provided evidence for reversible PKC-ϵ anchoring with binding and unbinding rates in the minute time domain. To independently confirm these observations, we monitored the development or loss of striations over time after mixing in or washing out PKC-ϵ-GFP. Fig. 4 illustrates a representative time course of fluorescence changes in a myocyte after rapid introduction of 160 nM PKC-ϵ-GFP into the chamber. The extracellular (bath) fluorescence changed from background to a maximum within one frame (30 s; not shown), but cell-associated fluorescence increased over several minutes. The striation pattern developed with a rate constant of 1.5×10^{-3} s^{-1} ($t_{1/2}$ = 7.7 min) as determined by fitting the data to a single-exponential function. Assuming the concentration of PKC-ϵ-GFP was constant throughout the binding process, we estimate a second-order rate constant of 1.5×10^{-3} s^{-1}/1.6×10^{-7} M = 9×10^3 M^{-1} s^{-1} for k_{on}. This k_{on} value is similar to what was measured by FRAP (Table 1).

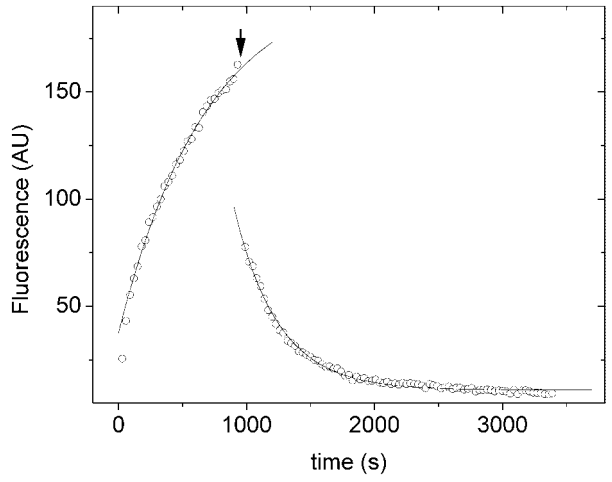

FIGURE 4 Time course of myocyte fluorescence changes during rapid mixing. Shown is the original record of fluorescence from a representative myocyte as activated PKC-ϵ-GFP (160 nM final concentration) was mixed into the chamber and then washed out (*arrow*) with fresh relaxing solution. The solid lines show fits to single-exponential equations. For the rising phase, the expression $y = y_o + a(1 - e^{-bx})$ was used, and the fitted value for b was $k_{on} = 9.1 \times 10^{-3}$ s^{-1}. For the declining phase, the expression $y = y_o + ae^{-bx}$ was used, and the fitted value for b was $k_{off} = 2.0 \times 10^{-3}$ s^{-1}. Mean values for k_{on} and k_{off} are compiled in Table 1.

TABLE 1 Summary of kinetic properties of PKC-ε and εV$_1$ binding in cardiac myocytes

	PKC-ϵ		ϵ-V1		
Constant	FRAP*	Perfusion†	FRAP*	Perfusion†	Steady state‡
k_{on}	$4.6 \pm 1.2 \times 10^3$ M^{-1} s^{-1}	$9.0 \pm 3 \times 10^3$ M^{-1} s^{-1}	$4.4 \pm 1.5 \times 10^3$ M^{-1} s^{-1}	$12 \pm 3 \times 10^3$ M^{-1} s^{-1}	
k_{off}	$0.75 \pm 0.1 \times 10^{-3}$ s^{-1}	$1.4 \pm 0.5 \times 10^{-3}$ s^{-1}	$1.3 \pm 0.3 \times 10^{-3}$ s^{-1}	$3.8 \pm 1.1 \times 10^{-3}$ s^{-1}	
K_d§	160 nM	150 nM	300 nM	330 nM	290 nM

*Rate constants ± SEM derived from linear regression fits of data in Fig. 3 *B* or 8 *B*.
†Rate constants derived from exponential fits of data as in Fig. 4. Data represent mean ± SEM for a minimum of four measurements from each of five separate cells.
‡Derived from a least-squares fit to data in Fig. 7 *C*.
§Calculated as the k_{off}/k_{on} ratio for each column. Errors are estimated to be ±30%.

We next established that PKC-ϵ binding near the Z-line was reversible by rapid addition of fresh relaxing solution while monitoring fluorescence intensity over time. Fluorescence in the bath surrounding the cells declined within one frame (15 s), showing that the solution change was rapid (not shown). The fluorescent striation pattern within the cell declined gradually over the course of hundreds of seconds, indicating slow unbinding of the probe (Fig. 4). This gradual loss of cell fluorescence was not caused by photobleaching, as it occurred independently of exposure to confocal laser illumination. The unbinding process followed an exponential decay of the form $y = y_o + ae^{-bx}$ where b is equivalent to k_{off}, the unbinding rate constant. The mean k_{off} compiled from multiple traces was $1.4 \pm 0.5 \times 10^{-3}$ s^{-1}, which translates to a half-time for PKC-ϵ dissociation of 8.3 min. This rate constant is within a factor of 2 of the k_{off} value determined by FRAP (Table 1).

Binding of ϵV1-GFP

To investigate which domains of PKC-ϵ might be responsible for anchoring to specific cardiac cell structures, we compared the binding of the N-terminal 144 amino acids, termed the ϵV_1 domain, with that of full-length PKC-ϵ. A typical image of ϵV_1-GFP-decorated myocytes is illustrated in Fig. 5. The striking cross-striated staining pattern evident in these images is similar to full-length PKC-ϵ-GFP. However, unlike the full-length construct, ϵV_1-GFP bound constitutively in the absence of any added activators. In addition, the ϵV_1-GFP pattern of fluorescence appears to be more discretely localized. This we believe is due to the fact that full-length enzyme exhibits more generalized association with intracellular membranes in addition to binding near the Z-line. Like PKC-ϵ-GFP, ϵV_1-GFP was concentrated on the Z-line, as evidenced by co-localization with the signature Z-line protein α-actinin (Fig. 6). In addition, the binding process for ϵV_1-GFP was found to be surprisingly slow ($t_{1/2} = 5$ min), as observed by mixing of cells with 200 nM ϵV_1-GFP and monitoring the development of striations over time. The ϵV_1-GFP probe also bound to myocytes reversibly, as the cross-striated pattern disappeared shortly ($t_{1/2} = 3$ min) after perfusing the chamber with relaxing solution (summarized in Table 1).

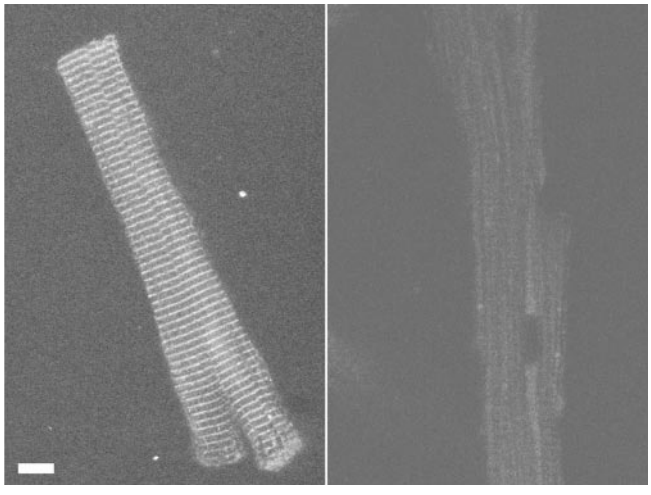

FIGURE 5 (*Left panel*) Laser scanning confocal micrograph of an isolated permeabilized myocyte incubated with GFP fused to the ϵV_1 region of PKC-ϵ; (*Right panel*) Autofluorescence of unstained myocytes at the same confocal microscope settings. Scale bar, 10 μm.

The isoform specificity of ϵV_1 binding, and by inference PKC-ϵ binding, was tested by use of the analogous 144-amino-acid N-terminal domain of PKC-δ, another novel PKC isozyme present in adult rat cardiac cells. The V_1 region of the δ isoform of PKC was fused to EGFP and expressed in DH5α cells and purified as a GST-fusion product. This construct did not exhibit the sarcomeric binding properties of ϵV_1-GFP but showed only low levels of diffuse staining (not shown). This observation illustrates the isoform selectivity of ϵV_1 anchoring near the Z-lines in cardiac cells. It also reinforces the control experiments performed with EGFP alone. Neither EGFP alone nor δV_1-GFP gave rise to a striated sarcomeric pattern of fluorescence demonstrating that the pattern observed with ϵV_1-GFP cannot be due to the simple process of filling t-tubules or other available volume within myocytes with the fluorescent probe.

As with full-length PKC-ϵ-GFP, the intensity of the striation pattern observed with ϵV_1-GFP varied with the concentration of applied probe. In this case due to the availability of higher concentrations of ϵV_1-GFP, it was possible to demonstrate saturation of binding. Fig. 7 shows a series of images of cells decorated with increasing concentrations of ϵV_1-GFP. Images such as these were quantitatively analyzed with a series of line-scan plots of pixel intensity versus position (Fig. 7 *B*). The heights of the peaks in this plot indicate the intensity of the striation pattern and are taken to represent the amount of ϵV_1-GFP bound at the Z-line. Fig. 7 *C* shows a plot of peak height versus [ϵV_1-GFP] that reveals a saturable binding relationship conforming to a hyperbolic fit of the form $y = ax/(b + x)$, where $b = K_d$. From this fit, we determined an apparent K_d of 290 ± 60 nM. The saturation observed was not due to a nonlinear response of the confocal microscope. Pixel counts of a rectangular region outside the cells being imaged demonstrated that the bath fluorescence continued to rise after saturation of the Z-line had occurred, until [ϵV_1-GFP] was well over 400 nM (Fig. 7 *C*).

FRAP measurements were also carried out with ϵV_1-GFP (Fig. 8). These measurements were consistent with reversible binding and with slow on and off rates for ϵV_1-GFP. k_{FRAP} was again found to depend upon the concentration of the GFP construct permitting estimates of k_{on} and k_{off}. The k_{on} value determined by FRAP was $4.4 \pm 1.5 \times 10^3$ M^{-1} s^{-1}, quite similar to the k_{on} measured for full-length PKC-ϵ-GFP. The k_{off} value for ϵV_1-GFP was $1.3 \pm 0.3 \times 10^{-3}$

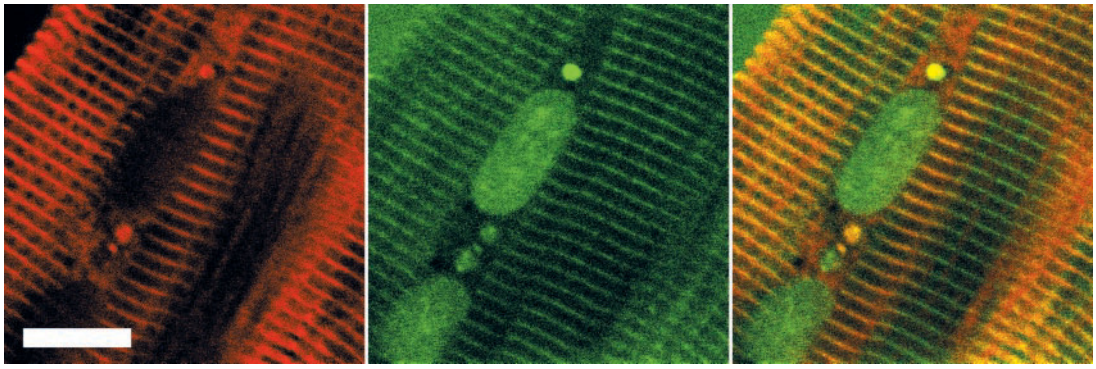

FIGURE 6 Co-localization of ϵV_1 domain with α-actinin. (*Left panel*) Confocal images of permeabilized myocytes decorated with monoclonal anti-α-actinin antibody and TRITC-labeled secondary antibodies in the red channel; (*Middle panel*) ϵV_1-GFP fusion construct in the green channel, showing a striated binding pattern (nuclear staining was not consistently observed); (*Right panel*) Areas of co-localization of ϵV_1-GFP and α-actinin appear as yellow in a red/green overlay.

s^{-1} or about twofold faster than for full-length PKC-ϵ-GFP. A detailed comparison of rate constants determined by wash-in/washout and by FRAP for the two GFP constructs is given in Table 1. In general, the data are compatible and present a consistent picture of the dynamics of PKC-ϵ binding to cardiac myocytes. Within a given method of measurement, on rates were very similar for ϵV_1-GFP and PKC-ϵ-GFP, and we take this as good evidence that ϵV_1 and PKC-ϵ-GFP binding have similar kinetic limits. Moreover, within a given method of measurement, off rates were consistently faster for ϵV_1-GFP (by two- to threefold) than for PKC-ϵ-GFP, and we take this as strong evidence that ϵV_1 binds more weakly and dissociates faster than does full-length PKC-ϵ. The sources of systematic errors that resulted in all FRAP-derived values being approximately twofold lower than those determined by perfusion may include photodamage to cells during photobleaching. Overall, the data provide a consistent picture of slow binding kinetics for PKC-ϵ that is mimicked by its ϵV_1 domain.

Values for K_d derived from rate constants are also presented in Table 1. Constraining k_{on} to be equivalent for both constructs, we arrive at a differences in K_d values due to different k_{off} values of twofold, the full-length enzyme being more slowly reversible and thus more tightly bound. Estimates for ϵV_1 derived from rate constants are in the range of 300–330 nM, and a steady state K_d value was independently measured to be 290 nM. By comparison, estimates for the K_d of full-length PKC-ϵ-GFP fall in the range of 150–160 nM. Thus, these dynamic measurements not only reveal slow binding and unbinding rates for PKC-ϵ anchoring to structures near the cardiac Z-line but also reveal a sub-micromolar affinity for this anchoring event.

DISCUSSION

The main findings of the present study are that PKC-ϵ binds in the vicinity of the cardiac Z-lines with binding and unbinding kinetics in the minute time domain. The observed on rate for binding measured by FRAP depended upon PKC-ϵ-GFP concentration with a slope equal to $\sim 9 \times 10^3$ M^{-1} s^{-1}. A similar slow on rate for PKC-ϵ-GFP binding was observed in mixing experiments. This value for k_{on} is at least two orders of magnitude less than a typical diffusion-controlled reaction rate for a protein of this size (Brown et al., 1999; Soumpasis, 1983). Thus, it appears that PKC-ϵ binding and by inference its translocation are inherently slow processes. The effective concentration of PKC-ϵ in vivo is unknown, but if we assume it is approximately equal to the K_d value estimated here, then this second-order on rate constant translates to a translocation half-time of 8 min. This value is similar to translocation time courses that have been reported previously in intact cells stimulated with agonists or lipid activators of PKC (Albert and Ford ,1999; Huang et al., 1997; Yoshida et al., 1996).

It is interesting to note that the binding of exogenous PKC-ϵ applied to permeabilized cells may be slow enough to account for the rate of onset of PKC-mediated positive inotropic responses in cardiac myocytes (Huang et al., 1996; Pi et al., 1997). This suggests that the slow binding kinetics are an intrinsic property of PKC-ϵ, because potential delays due to receptor activation, coupling to enzyme effectors such as phospholipase C, and second messenger formation/diffusion are absent from these measurements. Thus, it is possible that the cause of the delay between activation of PKC and its resulting effects may be entirely contained within the enzyme itself. Such a slow time course, which implies a large activation energy barrier in the binding of PKC-ϵ, may possibly be due to an unfolding of the protein structure or other obligatory intramolecular rearrangement. Perhaps binding of translocation activators induces slow conformational changes that ultimately expose the binding surface to its matched anchor and allow accumulation of PKC-ϵ at the Z-line. Mochly-Rosen and colleagues have suggested an auto-inhibitory mechanism wherein the an-

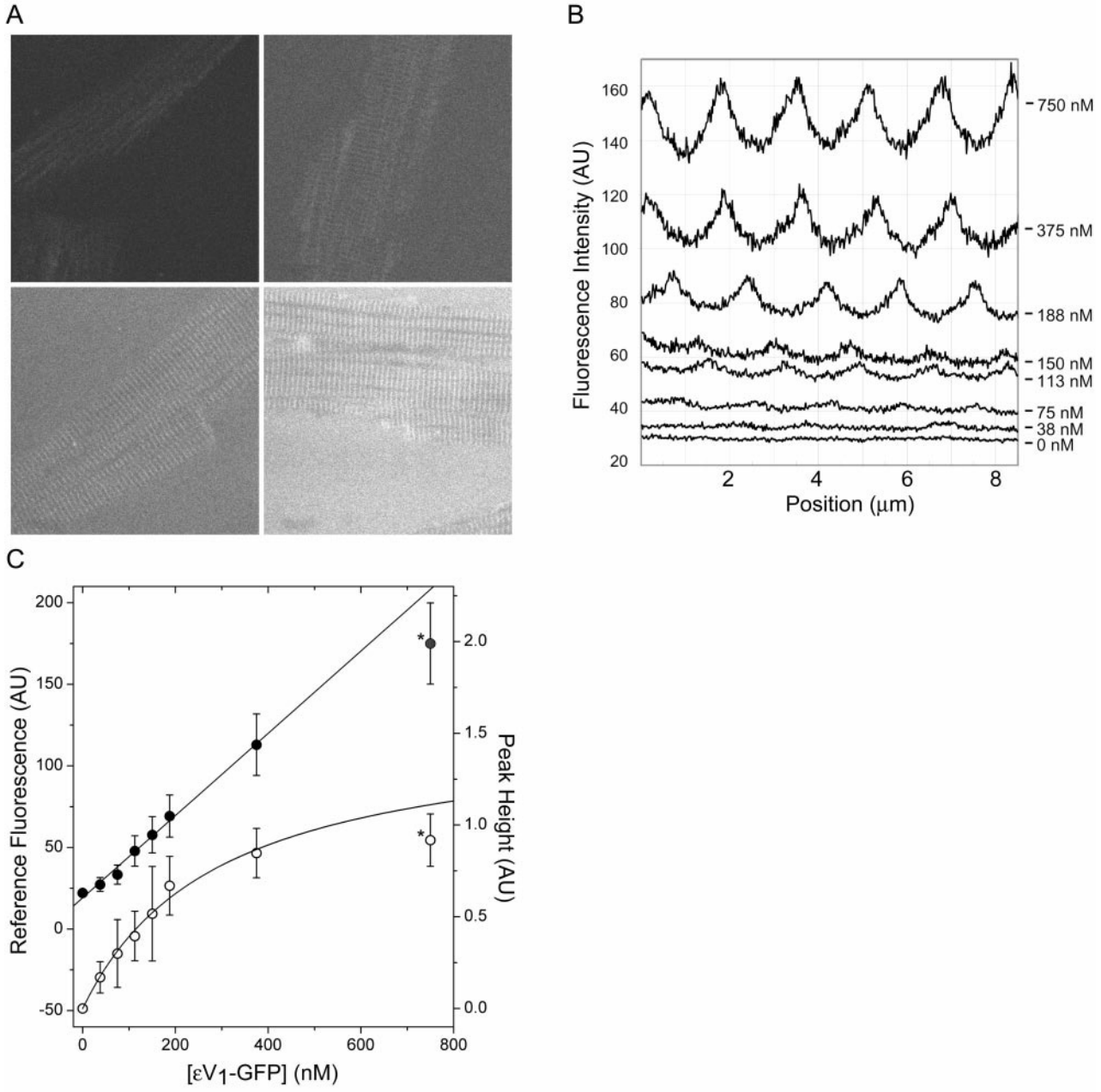

FIGURE 7 Concentration dependence of ϵV_1-GFP binding to permeabilized myocytes. (*A*) A series of confocal images of permeabilized myocytes decorated with increasing concentrations of ϵV_1-GFP; (*B*) Line-scan quantification of Z-line fluorescence. The height of the peaks corresponds to striation intensity, which increases with increasing [ϵV_1-GFP]. Interpeak distance represents sarcomere length, 1.7 μm. (*C*) Quantification of ϵV_1-GFP binding to myocytes based upon peak heights (○, *right axis*). The regression line represents a least-squares fit to a hyperbolic saturation curve with a K_d of 290 ± 60 nM. Average pixel intensity of a rectangular reference region outside the cell (●, *left axis*) demonstrates the linear response of the confocal microscope at this level of fluorescence. Points marked with an asterisk were considered to be outside of the linear response range and were not included in the regression analyses. Data represent mean ± SD.

chor-binding region of the regulatory domain of PKC-ϵ is obscured until translocation is stimulated (Dorn et al., 1999). This is analogous to the auto-inhibition of the catalytic domain of PKC by the pseudo-substrate region.

Much about the translocation and anchoring of PKC-ϵ is unknown. Indeed, a critical question that has not been definitively answered is the identity of the binding partner that anchors PKC after translocation. Some researchers have suggested that PKC interacts primarily with the surface of the phospholipid membrane, whereas others have proposed protein-binding partners. For example, Cypher-1, a PDZ domain-containing protein, has been shown to bind both

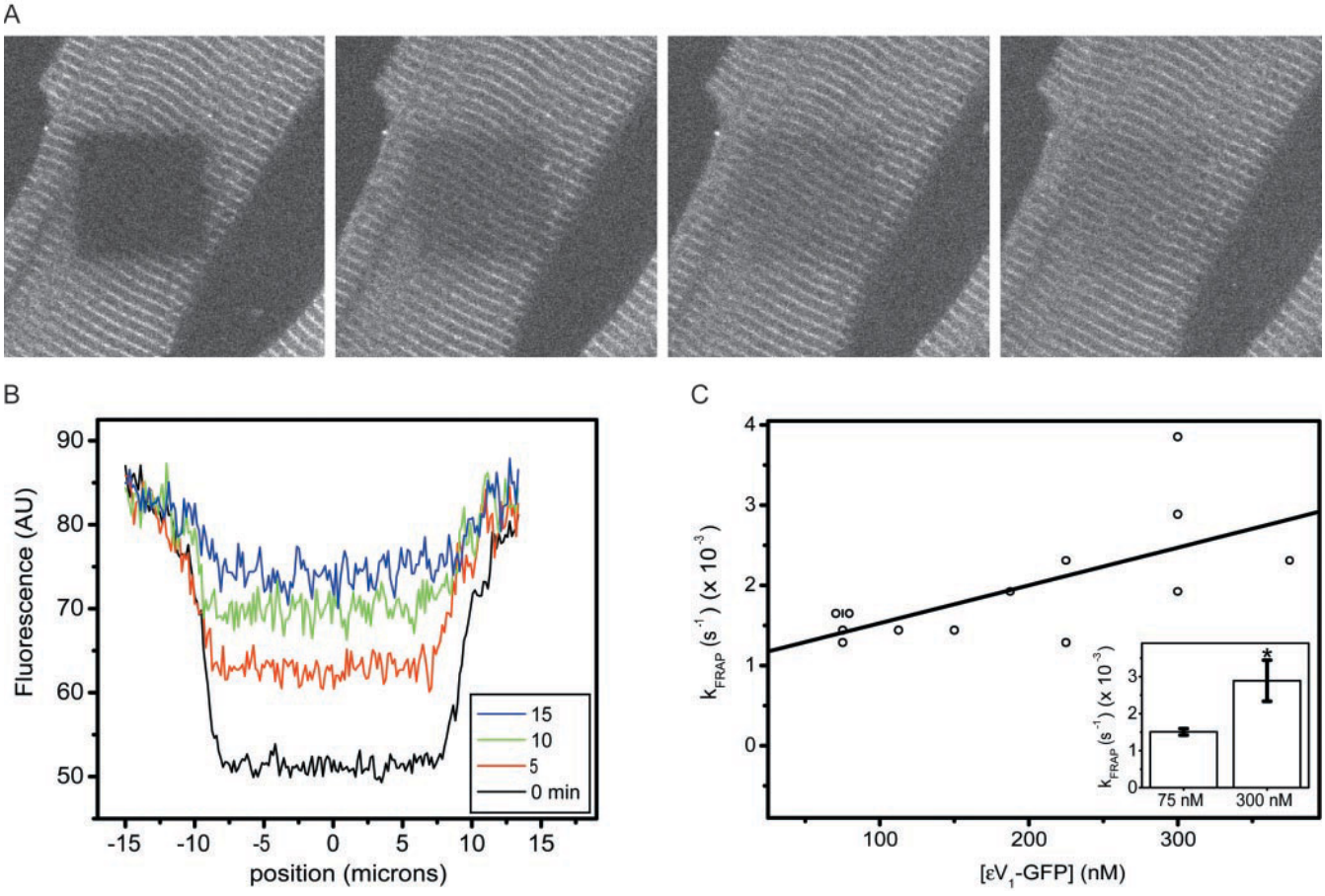

FIGURE 8 Photobleaching recovery of ϵV_1-GFP-decorated myocytes. (*A*) A permeabilized myocyte equilibrated with 150 nM ϵV_1-GFP was photobleached in a 16 × 16 μm square. Recovery of fluorescence is shown here at 0, 5, 10, and 15 min. (*B*) A line-scan quantification of fluorescence intensity versus position across the bleached region shows a uniform recovery of fluorescence over time. (*C*) Rate of photobleaching recovery, k_{FRAP}, depends upon the concentration of applied probe. Linear regression analysis gives a slope, $k_{on} = 4.4 \pm 1.5 \times 10^3$ M^{-1} s^{-1}, and a *y*-intercept, $k_{off} = 1.3 \pm 0.3 \times 10^{-4}$ s^{-1}. Overlapping data are offset. (*Inset*) Mean k_{FRAP} values ± SEM at low (75 nM) and high (300 nM) concentrations of PKC-ϵ-GFP. Data are represented as mean ± SEM; asterisk indicates statistical significance with $p < 0.05$.

α-actinin and several isoforms of PKC including PKC-ϵ (Zhou et al., 1999). Other possibilities include isoform-specific receptors for activated C kinase (RACKs) (reviewed in Mochly-Rosen, 1995) or docking structures such as caveolae (Rybin et al., 1999). F-actin has also been implicated in PKC anchoring (Prekeris et al., 1996), although peptide inhibition studies revealed that PKC-ϵ anchoring in Triton-X-100-skinned cardiac cells occurs through its V_1 domain rather than through its recognition motif for F-actin (Huang and Walker, 1997).

The ratio of the rate constants estimated in this study gives a dissociation constant for PKC-ϵ binding of ~150 nM (Table 1). This is similar to the K_d value of 90 nM obtained in a centrifugation binding assay using skinned cardiac myocytes (Huang and Walker, 1997). Previously there have been few estimates for the apparent affinity of PKC for its putative anchoring sites. The most thoroughly investigated anchor for PKC-ϵ is RACK2, which is fully saturated with PKC-ϵ in an in vitro assay at 10 nM (Csukai et al., 1997). A K_d value of ~1 nM is feasible for such an anchoring protein, if the protein ligand binds with a typical diffusion-controlled on rate of 10^6 to 10^7 M^{-1} s^{-1}. However, such a high affinity is not compatible with the much slower on rates estimated here. For example, if one assumes a simple binding mechanism, $k_{off} = K_d \times k_{on}$, then a high affinity (1 nM) and slow on rate (10^4 M^{-1} s^{-1}) would result in an unreasonably slow off rate (half-time > 19 h). Thus, the affinity for PKC-ϵ in cardiac myocytes in situ may be significantly lower than what has been measured for RACK2 in vitro (Csukai et al., 1997). Perhaps other proteins in the intracellular environment modulate the affinity of PKC-ϵ for RACK2. Alternatively, there may be multiple classes of anchoring sites with differing affinities and characteristic binding kinetics.

As mentioned above, a slow on rate of 9×10^3 M^{-1} s^{-1} ($t_{1/2}$ = 8 min at 150 nM PKC-ϵ) accounts for the time course of PKC-ϵ translocation as well as the onset of PKC-dependent responses (Huang et al., 1997; Pi et al., 1997).

The experimentally determined off rate of 1×10^{-3} s^{-1} ($t_{1/2}$ = 11 min) is also consistent with the time course of recovery from PKC-dependent responses (He et al., 2000; Pi et al., 1997). In addition, the observed on and off rates are compatible with the time course of ischemic preconditioning, which typically takes 5–15 min to develop and lasts 30–90 min (Lawson and Downey, 1993). Thus, it is possible that the window of protection provided by ischemic preconditioning is defined in part by the inherently slow binding and unbinding of activated PKC-ϵ.

Previously, several domains of PKC have been suggested to be important for translocation and anchoring in vivo. The C_1 region is known to mediate an avid membrane interaction when bound to diacylglycerol or phorbol esters. These PKC activators significantly increase the enzyme's membrane affinity, probably by contributing to a hydrophobic surface of C_1 (Zhang et al., 1995). This role for C_1 is supported by our data, because the full-length PKC-ϵ-GFP construct, which contains the C_1-domain, seems to bind more effectively to membrane structures than does ϵV_1-GFP, producing a staining pattern typical of a membrane-binding probe characterized by longitudinal streaks and perinuclear staining. We have consistently observed intense PKC-ϵ-GFP decoration of the conical, membrane-rich regions flanking the nucleus. It is unclear whether this is a generalized membrane-binding phenomenon or a specific receptor-mediated interaction of the sort shown for PKC-ϵ binding to Golgi in vitro (Csukai et al., 1997).

In a comprehensive study of the kinetics of translocation of PKC-γ in cultured RBL cells, Oancea and Meyer (1998) demonstrated a rapid Ca^{2+}-dependent interaction between its C_2 domain and the cell membrane. Interestingly, PKC-γ could also be induced to undergo membrane association in the absence of Ca^{2+} if phorbol ester was the activating ligand. The time course of PKC-γ translocation was greatly slowed ($t_{1/2}$ = 4 min) under these conditions making the time frame similar to PKC-ϵ translocation described here in cardiac cells. Oancea and Meyer (1998) proposed that the slow kinetics were due to conformational changes in the regulatory domain that unmask the C_1 phorbol ester binding site making it available for a productive membrane interaction. In light of our observations with ϵV_1-GFP, we propose that the critical rate-determining conformational changes reside in the V_1 domain itself for PKC-ϵ. One may speculate that the in vivo anchoring of PKC is mediated by both V_1 and C_1 elements, acting simultaneously or sequentially to achieve specific receptor interactions as well as generalized membrane binding. Analogous cooperative binding interactions have been described for the C_1 and C_2 domains of conventional PKC isoforms (Medkova and Cho, 1999).

Other important issues include identifying the substrates that PKC-ϵ phosphorylates as a result of translocation and anchoring and establishing precisely how phosphorylation is transduced into the various PKC-mediated effects that have been widely observed. The fact that the ϵ-isoform of PKC ultimately binds at the Z-line is suggestive of a mechanism by which PKC might exert its effects in the heart. The Z-line and its adjacent structures have long been known to be involved in excitation-contraction (EC) coupling, and it seems clear that a kinase anchored on or near the Z-line would be strategically positioned to modulate several key players. First among these are the L-type calcium channels, which are located on the transverse tubules that penetrate the sarcolemma near the Z-line. These channels are closely aligned with ryanodine receptors (RyRs) at close appositions between the transverse tubule and sarcoplasmic reticulum, called dyad junctions. Together, the L-type channels and the RyR coordinate the release of calcium in response to sarcolemma depolarization and are the subjects of a variety of cardiac regulatory cascades. The L-type calcium channel, in particular, is a likely substrate for PKC-ϵ and has been shown to respond to photorelease of a caged form of the PKC activator dioctanoylglycerol with an increase in peak current (He et al., 2000). This increase in I_{Ca} is concentration dependent and blockable with the PKC inhibitor chelerythrine. Consequently, our observations of PKC-ϵ binding at the Z-line have implications for its role in contractility modulation via regulation of EC coupling.

We thank Professor Mitsuo Ikebe for providing the PKC-ϵ clone, Kara R. Kemnitz for creating and expressing the δV_1-GFP construct, and Dr. Kenneth S. Campbell for assistance with data analysis. We also greatly appreciate the helpful advice of Dr. Eugenia M. Jones. Imaging was performed at the Keck Center for Biological Imaging at the University of Wisconsin with the technical assistance of Lance A. Rodenkirch.

This work was supported by National Institutes of Health grant P01 HL04759 (J.W.W.) and a fellowship from the American Heart Association (S.L.R.).

REFERENCES

Albert, C. J., and D. A. Ford. 1999. Protein kinase C translocation and PKC-dependent protein phosphorylation during myocardial ischemia. *Am. J. Physiol*. 276:H642–H650.

Brown, E. B., E. S. Wu, W. Zipfel, and W. W. Webb. 1999. Measurement of molecular diffusion in solution by multiphoton fluorescence photobleaching recovery. *Biophys. J.* 77:2837–2849.

Cohen, M. V., C. P. Baines, and J. M. Downey. 2000. Ischemic preconditioning: from adenosine receptor of KATP channel. *Annu. Rev. Physiol.* 62:79–109.

Csukai, M., C. H. Chen, M. A. De Matteis, and D. Mochly-Rosen. 1997. The coatomer protein beta′-COP, a selective binding protein (RACK) for protein kinase C-epsilon. *J. Biol. Chem.* 272:29200–29206.

Disatnik, M. H., G. Buraggi, and D. Mochly-Rosen. 1994. Localization of protein kinase C isozymes in cardiac myocytes. *Exp. Cell Res.* 210: 287–297.

Dorn, G. W., II, M. C. Souroujon, T. Liron, C. H. Chen, M. O. Gray, H. Z. Zhou, M. Csukai, G. Wu, J. N. Lorenz, and D. Mochly-Rosen. 1999. Sustained in vivo cardiac protection by a rationally designed peptide that causes epsilon protein kinase C translocation. *Proc. Natl. Acad. Sci. U.S.A.* 96:12798–12803.

Endo, M., and M. Iino. 1980. Specific perforation of muscle cell membranes with preserved SR functions by saponin treatment. *J. Muscle Res. Cell Motil.* 1:89–100.

He, J. Q., Y. Pi, J. W. Walker, and T. J. Kamp. 2000. Endothelin-1 and photoreleased diacylglycerol increase L-type Ca^{2+} current by activation of protein kinase C in rat ventricular myocytes. *J. Physiol. (Lond.).* 524:807–820.

Huang, X. P., Y. Pi, A. J. Lokuta, M. L. Greaser, and J. W. Walker. 1997. Arachidonic acid stimulates protein kinase C-epsilon redistribution in heart cells. *J. Cell Sci.* 110:1625–1634.

Huang, X. P., R. Sreekumar, J. R. Patel, and J. W. Walker. 1996. Response of cardiac myocytes to a ramp increase of diacylglycerol generated by photolysis of a novel caged diacylglycerol. *Biophys. J.* 70:2448–2457.

Huang, X. P., and J. W. Walker. 1997. Filamentous actin is not a PKC-ϵ anchoring protein in cardiac myocytes. *Mol. Biol. Cell.* 8:376a. (Abstr.)

Jaken, S. 1996. Protein kinase C isozymes and substrates. *Curr. Opin. Cell Biol.* 8:168–173.

Kawamura, S., K. Yoshida, T. Miura, Y. Mizukami, and M. Matsuzaki. 1998. Ischemic preconditioning translocates PKC-delta and -epsilon, which mediate functional protection in isolated rat heart. *Am. J. Physiol.* 275:H2266–H2271.

Kiley, S. C., S. Jaken, R. Whelan, and P. J. Parker. 1995. Intracellular targeting of protein kinase C isoenzymes: functional implications. *Biochem. Soc. Trans.* 23:601–605.

Lawson, C. S., and J. M. Downey. 1993. Preconditioning: state of the art myocardial protection. *Cardiovas.c Res.* 27:542–550.

Medkova, M., and W. Cho. 1999. Interplay of C1 and C2 domains of protein kinase C-alpha in its membrane binding and activation. *J. Biol. Chem.* 274:19852–19861.

Mochly-Rosen, D. 1995. Localization of protein kinases by anchoring proteins: a theme in signal transduction. *Science.* 268:247–251.

Murry, C. E., R. B. Jennings, and K. A. Reimer. 1986. Preconditioning with ischemia: a delay of lethal cell injury in ischemic myocardium. *Circulation.* 74:1124–1136.

Nishizuka, Y. 1992. Intracellular signaling by hydrolysis of phospholipids and activation of protein kinase C. *Science.* 258:607–614.

Oancea, E., and T. Meyer. 1998. Protein kinase C as a molecular machine for decoding calcium and diacylglycerol signals. *Cell.* 95:307–318.

Ono, Y., T. Fujii, K. Igarashi, T. Kuno, C. Tanaka, U. Kikkawa, and Y. Nishizuka. 1989. Phorbol ester binding to protein kinase C requires a cysteine-rich zinc-finger-like sequence. *Proc. Natl. Acad. Sci. U.S.A.* 86:4868–4871.

Papadopoulos, S., K. D. Jurgens, and G. Gros. 2000. Protein diffusion in living skeletal muscle fibers: dependence on protein size, fiber type, and contraction. *Biophys. J.* 79:2084–2094.

Pi, Y., R. Sreekumar, X. Huang, and J. W. Walker. 1997. Positive inotropy mediated by diacylglycerol in rat ventricular myocytes. *Circ. Res.* 81: 92–100.

Ping, P., J. Zhang, Y. Qiu, X. L. Tang, S. Manchikalapudi, X. Cao, and R. Bolli. 1997. Ischemic preconditioning induces selective translocation of protein kinase C isoforms epsilon and eta in the heart of conscious rabbits without subcellular redistribution of total protein kinase C activity. *Circ. Res.* 81:404–414.

Prekeris, R., M. W. Mayhew, J. B. Cooper, and D. M. Terrian. 1996. Identification and localization of an actin-binding motif that is unique to the epsilon isoform of protein kinase C and participates in the regulation of synaptic function. *J. Cell. Biol.* 132:77–90.

Qiu, Y., P. Ping, X. L. Tang, S. Manchikalapudi, Z. Rizvi, J. Zhang, H. Takano, W. J. Wu, S. Teschner, and R. Bolli. 1998. Direct evidence that protein kinase C plays an essential role in the development of late preconditioning against myocardial stunning in conscious rabbits and that epsilon is the isoform involved. *J. Clin. Invest.* 101:2182–2198.

Rybin, V. O., and S. F. Steinberg. 1994. Protein kinase C isoform expression and regulation in the developing rat heart. *Circ. Res.* 74:299–309.

Soumpasis, D. M. 1983. Theoretical analysis of fluorescence photobleaching recovery experiments. *Biophys. J.* 41:95–97.

Swaminathan, R., C. P. Hoang, and A. S. Verkman. 1997. Photobleaching recovery and anisotropy decay of green fluorescent protein GFP-S65T in solution and cells: cytoplasmic viscosity probed by green fluorescent protein translational and rotational diffusion. *Biophys. J.* 72:1900–1907.

Wang, Y., and M. Ashraf. 1998. Activation of alpha1-adrenergic receptor during Ca^{2+} pre-conditioning elicits strong protection against Ca^{2+} overload injury via protein kinase C signaling pathway. *J. Mol. Cell. Cardiol.* 30:2423–2435.

Ward, W., H. Prentice, A. Roth, C. Cody, and S. Reeves. 1982. Spectral perturbations of the *Aequorea* green-fluorescent protein. *Photochem. Photobiol.* 35:803–808.

Yoshida, K., T. Hirata, Y. Akita, Y. Mizukami, K. Yamaguchi, Y. Sorimachi, T. Ishihara, and S. Kawashiama. 1996. Translocation of protein kinase C-alpha, delta and epsilon isoforms in ischemic rat heart. *Biochim. Biophys. Acta.* 1317:36–44.

Zhang, G., M. G. Kazanietz, P. M. Blumberg, and J. H. Hurley. 1995. Crystal structure of the cys2 activator-binding domain of protein kinase C delta in complex with phorbol ester. *Cell.* 81:917–924.

Zhou, Q., P. Ruiz-Lozano, M. E. Martone, and J. Chen. 1999. Cypher, a striated muscle-restricted PDZ and LIM domain-containing protein, binds to alpha-actinin-2 and protein kinase C. *J. Biol. Chem.* 274: 19807–19813.